Front. Struct. Civ. Eng. 2022, 16(3): 378–387
https://doi.org/10.1007/s11709-022-0808-2

RESEARCH ARTICLE

Stability analysis of layered slopes in unsaturated soils

Guangyu DAI[a,b], Fei ZHANG[a,b*], Yuke WANG[c]

[a] *Key Laboratory of Ministry of Education for Geomechanics and Embankment Engineering, Hohai University, Nanjing 210098, China*

[b] *Jiangsu Province's Geotechnical Research Center, Nanjing 210098, China*

[c] *College of Water Conservancy Engineering, Zhengzhou University, Zhengzhou 450001, China*

[*] *Corresponding author. E-mail: feizhang@hhu.edu.cn*

ABSTRACT This study presents stability analyses of layered soil slopes in unsaturated conditions and uses a limit equilibrium method to determine the factor of safety involving suction stress of unsaturated soil. One-dimensional steady infiltration and evaporation conditions are considered in the stability analyses. An example of a two-layered slope in clay and silt is selected to verify the used method by comparing with the results of other methods. Parametric analyses are conducted to explore the influences of the matric suction on the stability of layered soil slopes. The obtained results show that larger suction stress provided in unsaturated clay dominates the stability of the layered slopes. Therefore, the location and thickness of the clay layer have significant influences on slope stability. As the water level decreases, the factor of safety reduces and then increases gradually in most cases. Infiltration/evaporation can obviously affect the stability of unsaturated layered slopes, but their influences depend on the soil property and thickness of the lower soil layer.

KEYWORDS slope stability, suction stress, unsaturated soil, layered slope, limit equilibrium

1 Introduction

Stability analyses of soil slopes is one of the most fundamental topics in geotechnical engineering. Most stability evaluations of slopes focus on completely dry or saturated condition, but the actual slopes are usually in unsaturated conditions. Rainfall-induced slope instability [1,2] and landslides of unsaturated residual soil [3,4] are closely related to changes of soil saturation. The stability analyses of unsaturated slopes become more important in many cases with the development of measurement technology.

Fredlund and Rahardjo [5] earlier proposed the independent stress state variable approach to evaluate the shear strength of unsaturated soil. Subsequently, Lu and Likos [6] used the soil-water characteristic curve (SWCC) and the effective shear strength parameters to characterize change of shear strength in unsaturated soil. The effects of suction stress based on their theory of unsaturated soil are involved in stability analyses of homogeneous slopes. Vahedifard et al. [7] adopted the log-spiral failure mechanism and presented a limit equilibrium (LE) method to assess the stability of unsaturated slopes subjected to one-directional (vertical) flow. Sun et al. [8] and Wang et al. [9] extended the method to consider the tension cracks and three-dimensional effects in stability evaluations of unsaturated slopes. Yang and Deng [10] considered the suction stress in the stability analyses of unsaturated slopes reinforced with piles. Their studies are limited to the unsaturated slopes in homogeneous soils. However, natural soils are usually layered due to sedimentation processes. It is worth noting that the matric suction could vary in different soils. Only a few studies [11,12] consider the conditional spatial variability in unsaturated soils, rather than investigate the effect of suction stress in different soil on the stability of an unsaturated layered slope. Most classical approaches for analyzing the layered slope stability are performed under dry or saturated conditions. The methods to evaluate the stability of layered soil slopes include LE method [13], upper-bound limit analysis method [14], and numerical finite-element

Article history: Received Sep 10, 2021; Accepted Dec 12, 2021

method [15–17]. These methods do not sufficiently take into account the effects of suction stress when solving for the safety factor of layered slopes. Moreover, few studies have been conducted to analyze the stability of unsaturated layered slopes using analytical approaches.

This study aims to investigate the influences of the matric suction on the stability of layered soil slopes under unsaturated conditions. The LE method using a generalized log-spiral slip surface is modified to involve suction stress and then to determine the factor of safety and the corresponding critical slip surface. The modified method is verified by comparing with the results published in literatures. A two-layered slope is used as an example to investigate the effects of soil property, layer thickness, groundwater level, and infiltration rate on the stability of unsaturated slopes.

2 Effective stress analyses and formulations

2.1 Definition of problem

A layered soil slope is analyzed under unsaturated conditions, as illustrated in Fig. 1. The thickness of each layer is H_i, and the interface between the soil layers is horizontal. The height and inclination angle of the slope are denoted as H and θ, respectively. The water table is located at H_w from the slope toe. For a positive value of H_w, the water level within the slope is equal to the reservoir level. When H_w is negative, the groundwater is below the toe, and no water pressure is acting on the slope surface. The soil below the water table is in a fully saturated state, while the soil above the water table is in an unsaturated state, which is beyond the capillary fringe regime. To determine the factor of safety for the presented slope, the following assumptions are made:

1) the soil for each layer is homogeneous and isotropic;

2) the Mohr–Coulomb failure criterion is adopted for each layered soil;

3) the potential slip surface passes through the toe of the slope;

4) the infiltration or evaporation rate is constant and the seepage may be considered to be in the vertical steady state;

5) the effect of capillary water is not significant here, and the soil above the water table is in unsaturated conditions;

6) tension cracks can be neglected.

2.2 Suction stress for unsaturated soils subjected to a steady flow

Based on Terzaghi's effective stress principle, Bishop [18] developed a stability analysis of slopes in unsaturated soils. The effective stress analysis is conducted here to solve the problem above. For unsaturated soils, matric suction plays an important role in shear strength change. A suction stress-based effective stress expression proposed by Lu and Likos [6,19] is employed for limit-equilibrium analyses of slope stability. As presented by Lu and Likos [19], a unified effective stress σ' is defined for both saturated and unsaturated conditions, as follows:

$$\sigma' = (\sigma - u_a) - \sigma^s, \tag{1}$$

where σ' and σ are the effective stress and the total stress, respectively; u_a is the pore-air pressure and σ^s is the

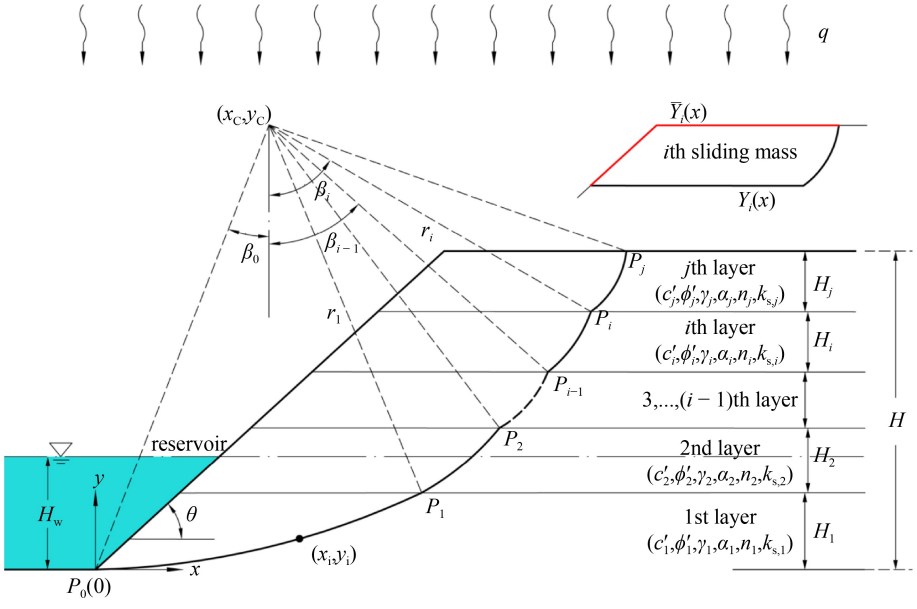

Fig. 1 Modeling of unsaturated slope stability analysis.

suction stress. Lu et al. [20] proposed closed-form equations for suction stress as a function of matric suction:

$$(u_a - u_w) \leqslant 0: \ \sigma^s = -(u_a - u_w), \tag{2a}$$

$$(u_a - u_w) \geqslant 0: \ \sigma^s = -\frac{(u_a - u_w)}{\{1 + [\alpha (u_a - u_w)]^n\}^{(n-1)/n}}, \tag{2b}$$

where u_w is pore water pressure; n and α are parameters fitting the SWCC and can be obtained from the SWCC model [21,22]. The parameter n is used to describe the distribution of the size of soil pore. The parameter α is equal to the inverse of the air-entry pressure value. When $u_a - u_w \leqslant 0$, the soil is in saturated conditions as shown in Eq. (2a). Lu et al. [23] conducted a series of experiments to verify the continuity and smoothness from Eq. (2b) to Eq. (2a), as the soil approaches saturation from the unsaturated state, using data from SWCC and suction stress characteristic curves (SSCC).

When a constant infiltration/evaporation flow is acting at the slope surface, an analytical solution for the matric suction $(u_a - u_w)$ under one-dimensional steady flow conditions was obtained by Lu and Likos [19] as follows:

$$(u_a - u_w) = -\frac{1}{\alpha} \ln \left[\left(1 + \frac{q}{k_s}\right) e^{-\alpha \gamma_w z} - \frac{q}{k_s} \right], \tag{3}$$

where $q > 0$ represents the steady evaporation rate, $q < 0$ represents infiltration rate, $q = 0$ represents the no-flow state; k_s = the saturated hydraulic conductivity; γ_w = the unit weight of water; z = the vertical distance from the water table to the critical sliding surface. Substituting Eq. (3) into Eq. (2b), the suction stress σ^s for soils under vertical steady-state conditions can be expressed as:

$$\sigma^s = -\frac{1}{\alpha} \frac{\ln \left[\left(1 + \frac{q}{k_s}\right) e^{-\alpha \gamma_w z} - \frac{q}{k_s} \right]}{\left\{ 1 + \left\{ -\ln \left[\left(1 + \frac{q}{k_s}\right) e^{-\alpha \gamma_w z} - \frac{q}{k_s} \right] \right\}^n \right\}^{(n-1)/n}}. \tag{4}$$

Equation (4) assumes that the suction stress varies only in the vertical direction and is constant in the horizontal plane. There is a limitation of Eq. (4) in that it cannot consider the possible effect of transient flow near the slope surface. With the simplified assumption of 1D vertical flow, the suction stress at different heights within the slope can be obtained from Eq. (4).

2.3 Limit equilibrium method using log-spiral slip surface

In the framework of LE method, using the generalized effective stress formula involving the suction stress in Eq. (1) can evaluate the stability of soil slopes in unsaturated conditions. The strength reduction method is employed here to determine the factor of safety for the unsaturated slopes and the factor of safety F_s is defined below

$$F_s = \frac{c'}{c'_m} = \frac{\tan \phi'}{\tan \phi'_m}, \tag{5}$$

where c' and ϕ' are the actual effective cohesion and internal friction angle of soil, respectively; c'_m and ϕ'_m represent the mobilized effective cohesion and friction angle. As presented by Stockton et al. [13], the log-spiral sliding surfaces can be used on layered soil slopes. This study extends the LE method from the uniform slope to the layered soil slope. A generalized log-spiral surface is adopted here. Considering the continuity of the log-spiral sliding surface in different soil layers, the sliding trace of a conventional homogeneous saturated/unsaturated soil slope needs to be modified as

$$r_i = A_i e^{-\beta_i \tan(\phi'_{m,i})} \ (1 \leqslant i - 1 \leqslant i \leqslant j), \tag{6}$$

where r_i = rotational radius of log-spiral surface for the ith soil layer; A_i = constant of the rotational radius; β_i = rotational angle from the vertical in different soil layer; $\phi'_{m,i}$ = the mobilized effective friction angle of the ith layered soil.

For layered soil slope, the log-spiral sliding surface of the first layer can be described by the two angles β_0 and β_1. The rotational radius constant A_1 can be calculated as

$$A_1 = -\frac{H_1}{e^{-\psi_{m,1}\beta_0} \cos \beta_0 - e^{-\psi_{m,1}\beta_1} \cos \beta_1}, \tag{7}$$

where $\psi_{m,i} = \tan \phi'_{m,i}$. The rotation center (x_c, y_c) can be determined by the bottom soil layer with initial radius A_1. The sliding surface is continuous in homogeneous soil layers, but breaks occur at the interface between the upper and lower soil layers, as shown in Fig. 1. To achieve a continuous sliding surface, the radiuses at the interface bewteen the $(i-1)$th and ith soil layers are identical and then the following relationship can be obtained:

$$A_{i-1} e^{-\psi_{m,i-1}\beta_{i-1}} = A_i e^{-\psi_{m,i}\beta_i}. \tag{8}$$

where A_{i-1} and A_i are the rotation radius constants of the $(i-1)$th and ith layer. Once the initial radius A_1 is calculated in Eq. (7), all of the constant $A_2, A_3, \ldots, A_j$ can be determined from Eq. (8).

The total stress σ is composed of the normal effective stress σ', pore-air pressure u_a, and suction stress σ^s from Eq. (1). For the generalized log-spiral surface, the LE moment equation around the rotational center can be explicitly written without specifying the normal stress over the slip surface. Because the direction of resultant force of σ' and its frictional component of the shear stress $\sigma' \tan \phi'$ at each point on the sliding surface always passes through the rotation center (x_c, y_c), as shown in Fig. 2.

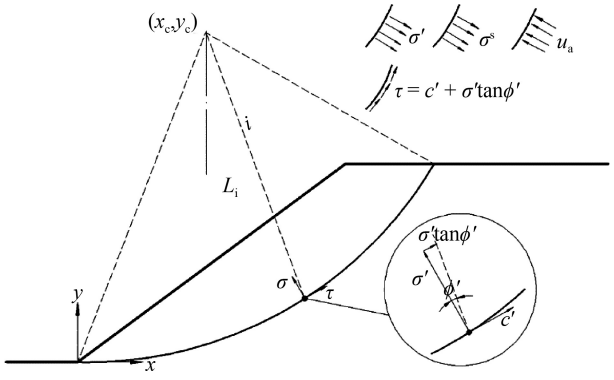

Fig. 2 Normal and shear stress acting on the log-spiral surface.

Therefore, the moment of σ' and $\sigma'\tan\phi'$ for the rotation center (x_c,y_c) is zero and not a concern in the following. The moments of u_a and σ^s need to be further determined, respectively. The LE moment equation around the rotation center (x_c,y_c) can be formulated as:

$$\sum_{i=1}^{n}(M_{G,i}+M_{\sigma^s,i}+M_{u_w,i}-M_{c'_{m,i}})-M_w=0, \tag{9}$$

where $M_{G,i}$ = moment of the self-weight gravity for the ith layer soil; $M_{\sigma^s,i}$ and $M_{u_w,i}$ = moments of the suction stress and the pore–water pressure, respectively; $M_{c'_{m,i}}$ = moment of the ith layer soil cohesion $c'_{m,i}$; M_w = moment of the water pressure acting on the slope surface ($M_w = 0$ if there is no water outside the slope).

The log spiral sliding surface is widely used in to assess the traditional slope stability. The relevant derivation process of the moment LE equation can be found in previous studies [24–26]. In the polar coordinates, with the geometry and notations in Fig. 1, the final expressions of $M_{G,i}$, $M_{u_w,i}$, $M_{\sigma^s,i}$, $M_{c'_{m,i}}$, M_w can be derived as:

$$M_{G,i}=\gamma_i\int_{\beta_{i-1}}^{\beta_i}(\bar{Y}_i(x)-Y_i(x))A_i e^{-\psi_{m,i}\beta}\sin\beta A_i e^{-\psi_{m,i}\beta}\left|\cos\beta-\psi_{m,i}\sin\beta\right|d\beta, \tag{10}$$

where γ_i = unit weight of the ith layered soil; $\bar{Y}_i(x)$ and $Y_i(x)$ represent equations of the upper and lower boundaries of the ith sliding body, as shown in Fig. 1.

The detailed procedure for solving $M_{G,i}$ is given in the Appendix.

$$M_{c'_{m,i}}=c'_{m,i}\int_{\beta_{i-1}}^{\beta_i}\left((-A_i e^{-\psi_{m,i}\beta}\cos\beta)-\frac{\psi_{m,i}\cos\beta+\sin\beta}{-\psi_{m,i}\sin\beta+\cos\beta}(A_i e^{-\psi_{m,i}\beta}\sin\beta)\right)(-\psi_{m,i}A_i e^{-\psi_{m,i}\beta}\sin\beta+A_i e^{-\psi_{m,i}\beta}\cos\beta)d\beta, \tag{11}$$

$$M_w=-\gamma_w H_w^2\left|A_1 e^{-\psi_{m,1}\beta_0}\cos(\beta_0-\theta)\right|-\frac{H_w}{6\sin^2\theta}, \tag{12}$$

when $y_i \geqslant H_w$:

$$M_{\sigma^s,i}=\int_{\beta_{i-1}}^{\beta_i}\sigma^s\cdot A_i e^{-\psi_{m,i}\beta}\cos\beta(A_i\psi_{m,i}e^{-\psi_{m,i}\beta}\cos\beta+A_i e^{-\psi_{m,i}\beta}\sin\beta)d\beta-\int_{\beta_{i-1}}^{\beta_i}\sigma^s\cdot A_i e^{-\psi_{m,i}\beta}\sin\beta(A_i\psi_{m,i}e^{-\psi_{m,i}\beta}\cos\beta-A_i e^{-\psi_{m,i}\beta}\sin\beta)d\beta, \tag{13}$$

$$M_{u_w,i}=0, \tag{14}$$

when $y_i \leqslant H_w$:

$$M_{\sigma^s,i}=0, \tag{15}$$

$$M_{u_w,i}=\gamma_w\int_{\beta_{i-1}}^{\beta_i}\psi_{m,i}(H_w-y_c+A_i e^{-\psi_{m,i}\beta}\cos\beta)\frac{A_i e^{-\psi_{m,i}\beta}}{(\psi_{m,i}\sin\beta-\cos\beta)}d\beta. \tag{16}$$

The obtained LE moment equation can calculate the factor of safety through an optimization procedure, as shown in Fig. 3. Choosing a reasonable initial value (β_0, β_1) is efficient for finding the factor of safety. To search for various potential slip surfaces, the minimum value of F_s can be derived and the corresponding critical slip surface can be also determined.

3 Results and discussion

3.1 Verification of calculated results

The suction stress of unsaturated soil slope is closely

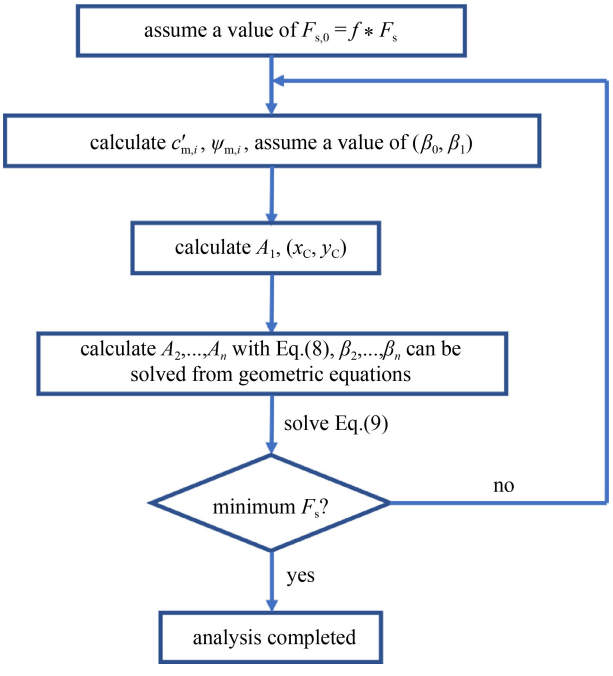

Fig. 3 Flow chart of the optimization procedure to determine the factor of safety.

related to the soil type and the extant environmental conditions. The representative values of soil parameters and hydraulic conditions of several typical soil bodies are given in Tables 1 and 2, respectively [7].

Vahedifard et al. [7] investigated the stability of the uniform slopes in unsaturated conditions and gave the cohesion needed to produce a LE state with $F_s = 1.0$. The presented analyses of unsaturated layered soil slope stability can assess the stability of the uniform slope. Here, the values of the required cohesion in Vahedifard et al. [7] are used to calculate the factor of safety, as shown in Table 3. It can be found that the factors of safety calculated by the presented method are very close to $F_s = 1.0$ as given in Vahedifard et al. [7]. The comparisons of the results can validate the accuracy of the presented method.

To further verify the applicability of the proposed method in estimating the stability of layered slopes, a two-layered slope with a height of 10 m is considered here. The thickness of each soil layer is 5 m. The soil properties of the two-layered soil are given in Table 4. Various slope angles are considered for calculations with suction and no suction. The Spencer LE method [27] is used to obtain the safety factors of the two-layered slopes without suction, as shown in Fig. 4. The results of this study are in good agreement with those derived by Spencer method. Once the matric suction is involved, the factor of safety obviously increases.

Table 1 The value of several typical unsaturated soil parameters [7]

soil type	φ' (°)	n	α (kPa^{-1})	k_s (m/s)
clay	20	2	0.005	5×10^{-8}
silt	25	3	0.010	5×10^{-7}
loess	28	4	0.025	1×10^{-6}
sand	30	5	0.100	3×10^{-5}

Table 2 Typical values of infiltration and evaporation rates [7]

flow type	q (m/s)
high infiltration	-3.14×10^{-8}
no flow	0
high evaporation	1.15×10^{-8}

Table 3 F_s for unsaturated slopes with the same soil properties in each layer

soil type	no suction	high infiltration	no flow	high evaporation
clay	1.017	1.002	1.000	1.002
silt	1.016	0.999	1.001	0.999
loess	1.002	1.001	0.999	1.001
sand	1.003	1.002	1.001	1.001

Table 4 Typical values of the unsaturated soil properties

soil type	n	α (kPa^{-1})	k_s (m/s)	ϕ' (°)	c' (kPa)	γ (kN/m^3)
clay	1.7	0.005	5×10^{-8}	20	10	18
silt	4.0	0.05	1×10^{-7}	30	5	18

3.2 Parametric analysis

Parametric studies are made using the two-layered slope, of which the soil parameters are given in Table 4. Figure 5 shows the SWCC and SSCC for clay and silt soils in this study.

3.2.1 Effect of layer thickness

A slope with $H = 10$ m is considered here without the vertical-specific discharge $q = 0$ and the water level is located at the slope toe. Figure 6 shows the factor of safety F_s versus the layer thickness for various slope ratios k (slope angle $\theta = \arctan k$). For the slope in Case 1, the upper and lower layers are clay and silt, respectively. In Case 2, the soil layers are in the opposite relative positions. Both saturated and unsaturated analyses are carried out to obtain the factor of safety for the two cases.

From the results, it can be seen that the layer thickness has minor influence on the stability of slopes in saturated soils, especially for steep slopes. The unsaturated

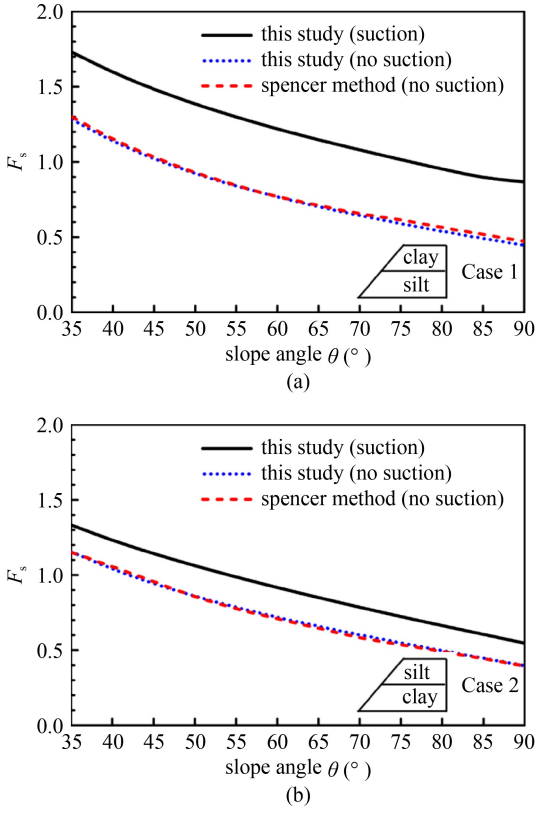

Fig. 4 Comparisons of F_s between the presented method and Spencer method for: (a) Case 1: the upper layer is clay and the lower layer is silt; (b) Case 2: the upper layer is silt and the lower layer is clay.

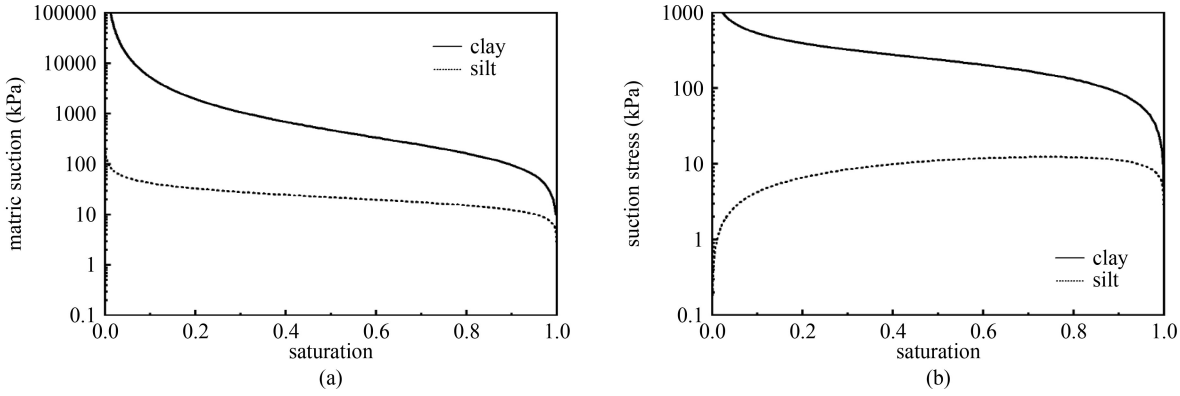

Fig. 5 (a) SWCC for clay and silt soils; (b) SSCC for clay and silt soils.

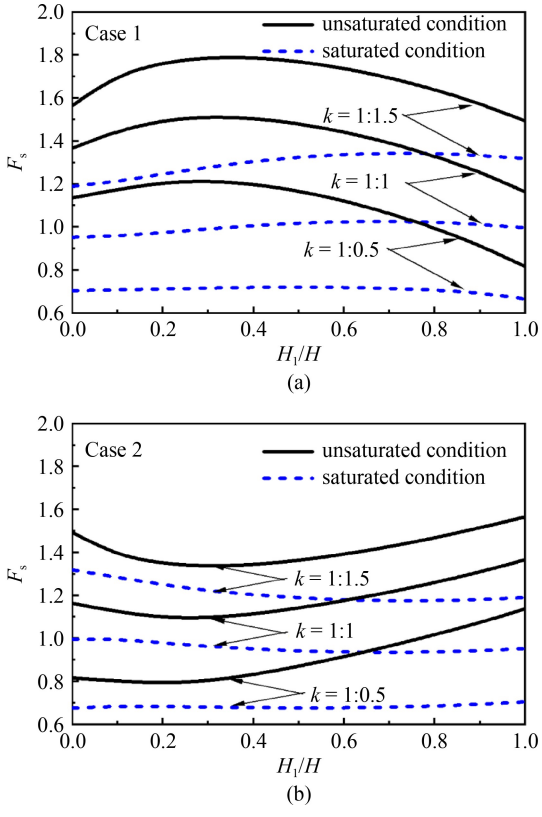

Fig. 6 Variation of F_s with the thickness of soil layer for: (a) Case 1: the upper layer is clay and the lower layer is silt; (b) Case 2: the upper layer is silt and the lower layer is clay.

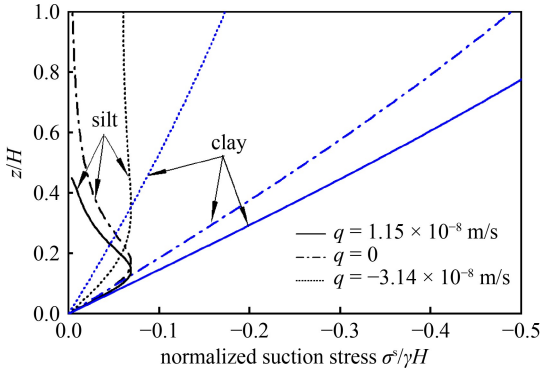

Fig. 7 Distribution of suction stress along vertical elevation of an unsaturated slope in uniform clay/silt (H = 10 m, H_w = 0).

conditions can affect the stability of slopes in layered soils. For an unsaturated slope of Case 1, its factor of safety increases with increasing ratio H_1/H and then reduces when the thickness of the lower layer $H_1 > 0.2H$. On the contrary, the unsaturated slope of Case 2 decreases as the ratio H_1/H increases and then increases. It implies that the unsaturated slope is more stable in Case 1 but less stable in Case 2 when the thickness H_1 approaches $0.2H$. The reason for this could be attributed to the contributions of the matric suction of clay or silt to the safety of unsaturated slopes in different soil thicknesses. Figure 7 illustrates the distribution of suction stress along with the height of an unsaturated slope in uniform clay or silt. The suction stress in clay increases linearly with the distance z above the water level. However, the suction stress in the silt increases when $z < 0.2H$, and then decreases gradually. In Case 1, as the thickness of silt in the lower layer exceeds $0.2H$, the suction stress of clay is the dominant influence on safety and its decrease makes the slope less stable. In Case 2, the suction stress in clay can provide more contributions to the resistances and then increase the slope stability. Therefore, the effects of the layer thickness on the stability of unsaturated slopes in layered soils are clear.

3.2.2 Effect of water level

In Case 1 and Case 2 for slopes without infiltration (q = 0), the influences of the groundwater level H_w on the factor of safety are investigated here. For a negative value of H_w, the slope is unsaturated. When the water level H_w is positive, the water level outside the slope is identical to that inside. Various water levels are considered in the calculations. Figure 8 illustrates variations with the water level of the factor of safety for the unsaturated layered slope. It can be seen that the water level has obvious impacts on the unsaturated slope stability. When the water level is above the slope toe, F_s decreases with

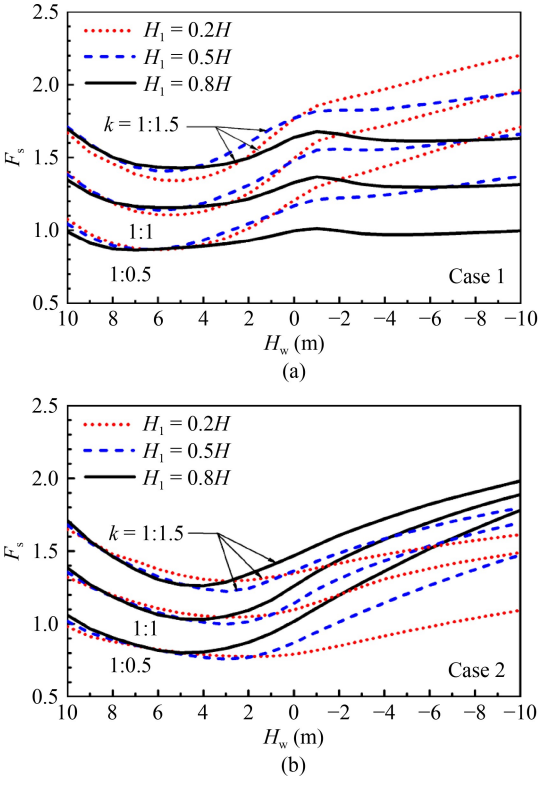

Fig. 8 Variation of F_s with water table level for: (a) Case 1: the upper layer is clay and the lower layer is silt; (b) Case 2: the upper layer is silt and the lower layer is clay.

increasing H_w and then gradually increases. When the water level is underneath the slope toe, the variations of F_s are different in the two cases. In Case 1, the F_s increases with the reducing H_w and then changes to reduce or slightly increase after the water level $H_w = -1$ m. In Case 2, F_s keep increasing with the water level.

For $H_w < 0$, the groundwater level is located below the slope toe. In this situation, the matric suction of the unsaturated soil makes more contributions to slope stability. Figure 9 illustrates the influences of the groundwater level on the critical sliding surface of Case1. As the water level H_w decreases, the critical slip surface becomes deeper but not obvious in the case of $H_1 = 0.8H$. Although the slip surface is deeper with the decreasing water level, the factor of safety increases after a minimum. That's due to the favorable effects of unsaturated suction stress. As shown in Fig. 7, more matric suction is provided if the clay layer is thicker. Therefore, the effect of the matric suction is significant on the unsaturated slope with a large clay layer (e.g., $H_1 = 0.2H$).

3.2.3 Effect of infiltration/evaporation rate

To investigate the influence of the infiltration/evaporation rate on the slope stability, the slope case with $\theta = 45°$ and $H_w = 0$ is considered here. Figure 10 gives the variation of the safety factor with the flow rate q for $H_1 = 0$, $0.25H$,

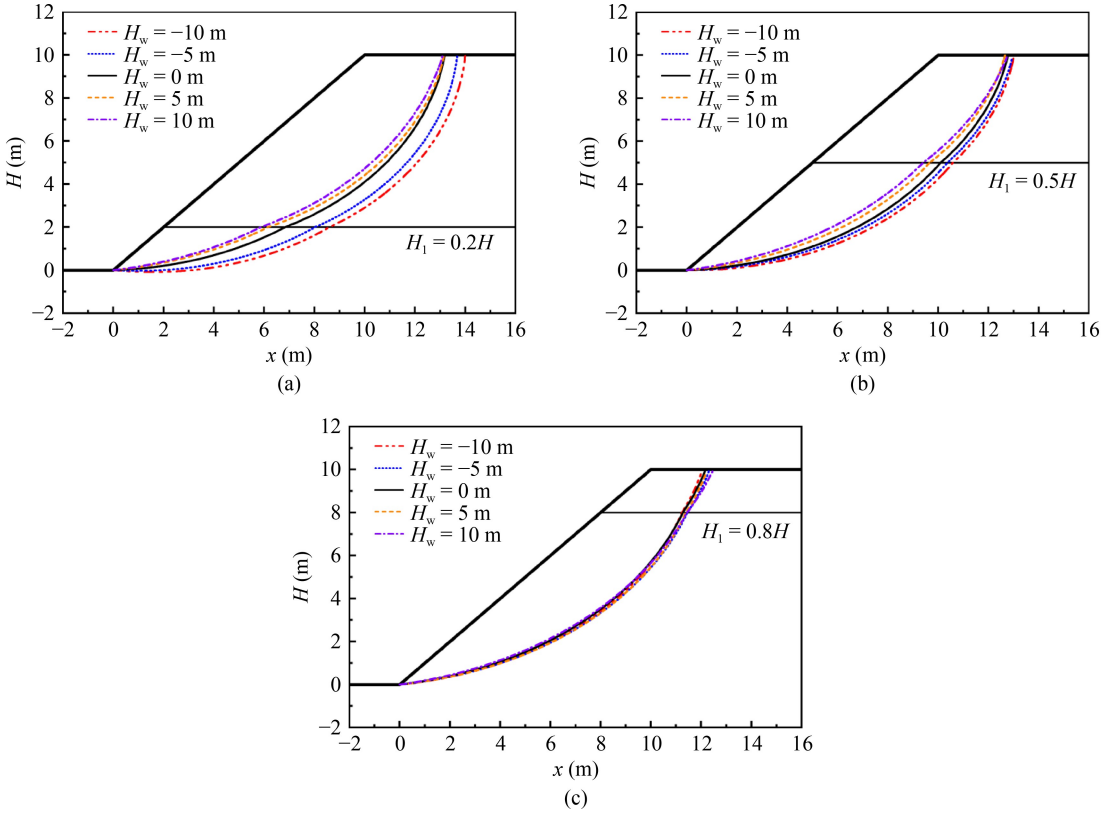

Fig. 9 Effects of the groundwater level on the critical sliding surface of Case 1 ($\theta = 45°$) with: (a) $H_1 = 0.2H$; (b) $H_1 = 0.5H$; (c) $H_1 = 0.8H$.

0.50H, 0.75H, and 1.00H. For $H_1 = 0$ and 1.00H, they are the homogeneous slopes in silt and clay soil, respectively. For the clay slope ($H_1 = 0$ in Case 1 or $H_1 = H$ in Case 2), the factor of safety increases with increasing q. On the contrary, the factor of safety for the silt slope ($H_1 = H$ in Case 1 or $H_1 = 0$ in Case 2) decreases as q increases. That's because matric suction for unsaturated clay is much larger than that in slit, as shown in Fig. 7 (the suction stress distribution). It can be seen that the suction stress in clay slope increases with increasing q, while it is opposite for the silt slope with vertical elevation greater than 0.2H. Especially for $q > 0$, there is no effect of suction stress acting on the silt slope when the slope elevation exceeds one-half height.

For the layered slope, the soil permeability k_s is not uniform. Infiltration/evaporation rates can vary for different layered soils at the same flow rate. Typical representative values of infiltration and evaporation rates are used, as shown in Table 2. For layered soil slope of Case 1, the factor of safety always increases with increasing q. But in Case 2 with $H_1 < 0.25H$, the F_s reduces as q increases. In this case, the matric suction due to silt was the dominant influence on stability of the unsaturated slope, and its safety decreases with q. Figure 11 gives the variation of the safety factor for a uniform slope with the ratio of permeability/evaporation rate and permeability $Q = q/k_s$. It can be seen that the F_s of clay slopes increases significantly with increasing Q. For silt slopes, F_s increases with the increase of Q and then reduces after $Q \geqslant -0.3$. There is no significant variation in F_s when $Q \geqslant 0.3$, indicating the evaporation rate has little effect on the suction stress of silt slopes. Figure 10 demonstrates that the slope stability tends to decrease with increasing q when the clay layer is thinner than the silt layer.

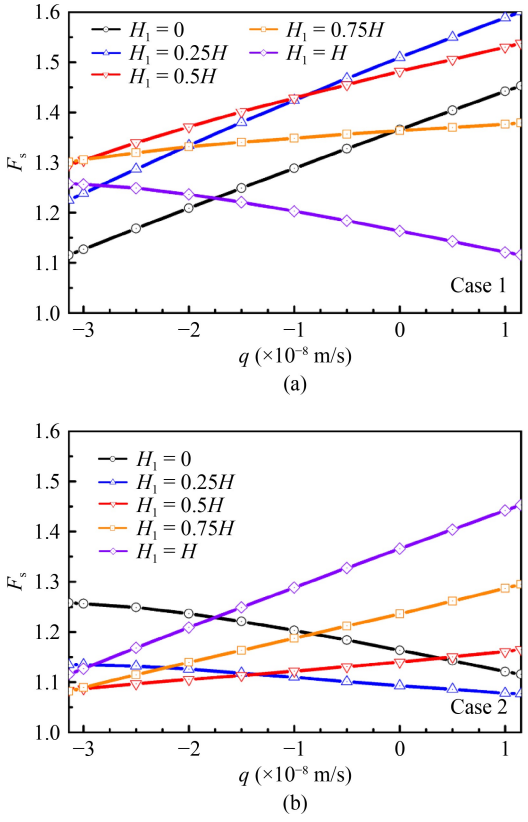

Fig. 10 Influence of the infiltration/evaporation rate on the factor of safety ($\theta = 45°$, $H_w = 0$) for (a) Case 1: the upper layer is clay and the lower layer is silt; (b) Case 2: the upper layer is silt and the lower layer is clay.

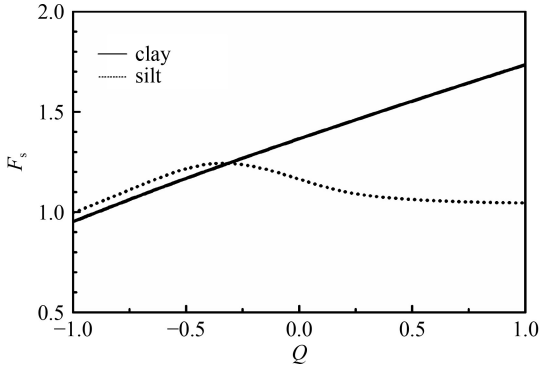

Fig. 11 Influence of the dimensionless infiltration/evaporation rate on the safety of the unsaturated slope in clay or silt ($\theta = 45°$, $H_w = 0$).

4 Conclusions

This paper extends the LE analysis of unsaturated slope stability from uniform soil to layered soil. It has been verified that the proposed analytical theory for the slope stability of unsaturated layered soils can also solve the problem for homogeneous slopes. A two-layered soil slope consisting of clay and silt is considered for calculations to investigate the effect of suction stress on the stability of the layered soil slopes. Parametric studies (e.g., layer distribution, soil layer thickness, groundwater level, and infiltration rate) are carried out, and some conclusions can be drawn below.

1) The contributions of the matric suction on the stability of unsaturated slopes in clay are more obvious than that in silt. The thickness of the soil layer has significant effects on the stability of layered soil slopes. For a two-layered slope in upper-layer clay and lower-layer silt, the safety factor decreases with increase of silt thickness when the thickness of the silt layer exceeds 0.2H. The opposite is the case for the two-layered slope in upper-layer silt and lower-layer clay.

2) When the groundwater level is located above the slope toe, the safety factor of the layered slope reduces and then increases as the water level decreases. When the water table is below the toe of the slope, the factor of safety increases with decreasing water level. However,

when the lower-layer soil is silt and thicker than the clay layer, the change of the water level below the slope toe has minor influence on the slope safety.

3) Infiltration/evaporation can obviously affect the stability of unsaturated layered slopes. The factor of safety increases with the increase of q, except when the lower-layer soil is clay and the thickness of the clay layer is less than $0.25H$.

Appendix

The soil properties of the layered slopes could affect the location of the potential sliding surface, which yields to the complexity of the calculation on the moment of the self-weight gravity, $M_{G,i}$. Here, a two-layered soil slope is considered as the typical example, as shown in Fig. A1. The intersection between the sliding surface and the horizontal interface of the layered soils is Point F, at which is the angle β_F. Point E is the projection of the crest Point X on the sliding surface and the corresponding angle is β_E. The total moment $M_{G,i}$ can be divided into five parts, i.e., $M_{G,1\text{-}1}$, $M_{G,1\text{-}2}$, $M_{G,2\text{-}1}$, $M_{G,2\text{-}2}$, and $M_{G,2\text{-}3}$.

The moments $M_{G,1\text{-}1}$ and $M_{G,1\text{-}2}$ for the first soil layer can be expressed as:

$$M_{G,1\text{-}1} = \gamma_1 \int_{\beta_C}^{\beta_D} (A_1 e^{-\psi_{m,1}\beta} \sin\beta \tan\theta + A_1 e^{-\psi_{m,1}\beta} \cos\beta) A_1^2 e^{-2\psi_{m,1}\beta} \sin\beta \left|\cos\beta - \psi_{m,1}\sin\beta\right| d\beta, \quad (A1)$$

$$M_{G,1\text{-}2} = \gamma_1 \int_{\beta_D}^{\beta_F} (H_1 - y_c + A_1 e^{-\psi_{m,1}\beta} \cos\beta) A_1^2 e^{-2\psi_{m,1}\beta} \sin\beta \left|\cos\beta - \psi_{m,1}\sin\beta\right| d\beta. \quad (A2)$$

The relationship between Points E and F can result in two cases of the calculations on the moment of the upper-layer, as below:

Case 1: $\beta_F > \beta_E$

$$M_{G,2\text{-}3} = \gamma_2 \int_{\beta_D}^{\beta_E} (A_1 e^{-\psi_{m,1}\beta} \sin\beta \tan\theta - H_1 + y_c) A_1^2 e^{-2\psi_{m,1}\beta} \sin\beta \left|\cos\beta - \psi_{m,1}\sin\beta\right| d\beta, \quad (A3)$$

$$M_{G,2\text{-}4} = \gamma_2 \int_{\beta_E}^{\beta_F} (H - H_1) A_1^2 e^{-2\psi_{m,1}\beta} \sin\beta \left|\cos\beta - \psi_{m,1}\sin\beta\right| d\beta, \quad (A4)$$

$$M_{G,2\text{-}5} = \gamma_2 \int_{\beta_F}^{\beta_B} (H - y_c + A_2 e^{-\psi_{m,2}\beta} \cos\beta) A_2^2 e^{-2\psi_{m,2}\beta} \sin\beta \left|\cos\beta - \psi_{m,2}\sin\beta\right| d\beta. \quad (A5)$$

Case 2: $\beta_F \leqslant \beta_E$

$$M_{G,2\text{-}3} = \gamma_2 \int_{\beta_D}^{\beta_F} (A_1 e^{-\psi_{m,1}\beta} \sin\beta \tan\theta - H_1 + y_c) A_1^2 e^{-2\psi_{m,1}\beta} \sin\beta \left|\cos\beta - \psi_{m,1}\sin\beta\right| d\beta, \quad (A6)$$

$$M_{G,2\text{-}4} = \gamma_2 \int_{\beta_F}^{\beta_E} (A_2 e^{-\psi_{m,2}\beta} \sin\beta \tan\theta + A_2 e^{-\psi_{m,2}\beta} \cos\beta) A_2^2 e^{-2\psi_{m,2}\beta} \sin\beta \left|\cos\beta - \psi_{m,2}\sin\beta\right| d\beta, \quad (A7)$$

$$M_{G,2\text{-}5} = \gamma_2 \int_{\beta_E}^{\beta_B} (H - y_c + A_2 e^{-\psi_{m,2}\beta} \cos\beta) A_2^2 e^{-2\psi_{m,2}\beta} \sin\beta \left|\cos\beta - \psi_{m,2}\sin\beta\right| d\beta. \quad (A8)$$

Acknowledgements This study was supported by the National Natural Science Foundation of China (Grant Nos. 52078185 and 51878248).

References

1. Clague J J, Stead D. Landslides: Types, Mechanisms and Modeling. New York: Cambridge University Press, 2012
2. Fuchu D, Lee C F, Sijing W. Analysis of rainstorm-induced slide-debris flows on natural terrain of Lantau Island, Hong Kong (China). Engineering Geology, 1999, 51(4): 279–290
3. Lu N, Wayllace A, Oh S. Infiltration-induced seasonally reactivated instability of a highway embankment near the Eisenhower Tunnel, Colorado, USA. Engineering Geology, 2013, 162: 22–32
4. Sorbino G, Nicotera M V. Unsaturated soil mechanics in rainfall-induced flow landslides. Engineering Geology, 2013, 165: 105–132

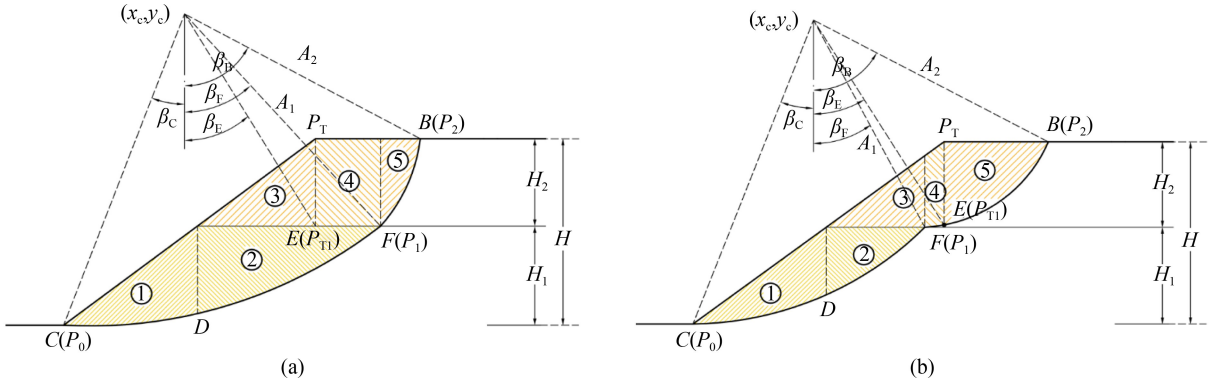

Fig. A1 Different calculations on the moment of the self-weight gravity when (a) $\beta_F > \beta_E$ and (b) $\beta_F \leqslant \beta_E$.

5. Fredlund D G, Rahardjo H. Soil Mechanics for Unsaturated Soils. Hoboken: John Wiley & Sons, Inc, 1993
6. Lu N, Likos W J. Suction stress characteristic curve for unsaturated soil. Journal of Geotechnical and Geoenvironmental Engineering, 2006, 132(2): 131−142
7. Vahedifard F, Leshchinsky D, Mortezaei K, Lu N. Effective stress-based limit-equilibrium analysis for homogeneous unsaturated slopes. International Journal of Geomechanics, 2016, 16(6): D4016003
8. Sun D A, Wang L, Li L. Stability of unsaturated soil slopes with cracks under steady-infiltration conditions. International Journal of Geomechanics, 2019, 19(6): 04019044
9. Wang L, Hu W, Sun D A, Li L. 3D stability of unsaturated soil slopes with tension cracks under steady infiltrations. International Journal for Numerical and Analytical Methods in Geomechanics, 2019, 43(6): 1184−1206
10. Yang M, Deng B. Stability study of slope reinforced with piles under steady unsaturated flow conditions. Computers and Geotechnics, 2019, 109: 89−98
11. Masoudian M S, Hashemi Afrapoli M A, Tasalloti A, Marshall A M. A general framework for coupled hydro-mechanical modelling of rainfall-induced instability in unsaturated slopes with multivariate random fields. Computers and Geotechnics, 2019, 115: 103162
12. Gholampour A, Johari A. Reliability-based analysis of braced excavation in unsaturated soils considering conditional spatial variability. Computers and Geotechnics, 2019, 115: 103163
13. Stockton E, Leshchinsky B, Xie Y, Olsen M J, Leshchinsky D. Limit equilibrium stability analysis of layered slopes: A generalized approach. Transportation Infrastructure Geotechnology, 2018, 5(4): 366−378
14. Kumar J, Samui P. Stability determination for layered soil slopes using the upper bound limit analysis. Geotechnical and Geological Engineering, 2006, 24(6): 1803−1819
15. Guo S, Li N, Liu W, Ma Z, Liu N, Lv G. Influence of both soil properties and geometric parameters on failure mechanisms and stability of two-layer undrained slopes. Advances in Materials Science and Engineering, 2020, 2020: 4253026
16. Lim K, Li A J, Lyamin A V. Three-dimensional slope stability assessment of two-layered undrained clay. Computers and Geotechnics, 2015, 70(OCT): 1−17
17. Wu G, Zhang R, Zhao M, Zhou S. Undrained stability analysis of eccentrically loaded strip footing lying on layered slope by finite element limit analysis. Computers and Geotechnics, 2020, 123: 103600
18. Bishop A W. The experimental study of partly saturated soil in the triaxial apparatus. In: 5th International Conference on Soil Mechanics & Foundation Engineering. Paris, 1961, 1: 13−21
19. Lu N, Likos W J. Unsaturated Soil Mechanics. Hoboken: John Wiley & Sons, Inc, 2004
20. Lu N, Godt J W, Wu D T. A closed-form equation for effective stress in unsaturated soil. Water Resources Research, 2010, 46(5): W05515
21. Vangenuchten M T. A closed-form equation for predicting the hydraulic conductivity of unsaturated soils. Soil Science Society of America Journal, 1980, 44(5): 892−898
22. Mualem Y. A new model for predicting the hydraulic conductivity of unsaturated porous media. Water Resources Research, 1976, 12(3): 513−522
23. Lu N, Kaya M, Collins B D, Godt J W. Hysteresis of unsaturated hydromechanical properties of a silty soil. Journal of Geotechnical and Geoenvironmental Engineering, 2013, 139(3): 507−510
24. Baker R, Garber M. Theoretical analysis of the stability of slopes. Geotechnique, 1978, 28(4): 395−411
25. Leshchinsky D. Short-term stability of reinforced embankment over clayey foundation. Soil and Foundation, 1987, 27(3): 43−57
26. Leshchinsky D. Slope stability analysis: Generalized approach. Journal of Geotechnical Engineering, 1990, 116(5): 851−867
27. Spencer E. A method of analysis of the stability of embankments assuming parallel inter-slice forces. Geotechnique, 1967, 17(1): 11−26